Substrate-dependent magnetization in Co-doped ZnO insulating films

C. Song, F. Zeng, K. W. Geng, X. J. Liu, and F. Pan*
Laboratory of Advanced Materials, Department of Materials Science and Engineering, Tsinghua University, Beijing 100084, People's Republic of China

B. He and W. S. Yan
National Synchrotron Radiation Laboratory, University of Science and Technology of China, Hefei 230029, People's Republic of China
(Received 1 September 2006; revised manuscript received 5 November 2006; published 19 July 2007)

Magnetization and local Co structure of 4 at. % Co-doped ZnO insulating films, prepared by direct current reactive magnetron cosputtering, have been studied as a function of substrates. Although all the Co:ZnO films possess a common feature that Co^{2+} replaces Zn^{2+}, room-temperature ferromagnetism of Co:ZnO films is strongly dependent on the substrates. The reorganization of defects due to magnetoelectric coupling and a slight dissimilarity among Co *K*-edge x-ray-absorption near-edge structure spectra on different substrates reveal that the combination of Co:ZnO film grown on ferroelectric substrates and a suitable Co-O bond length likely serves as a key in enhancing the magnetic ordering. Furthermore, electric property measurements demonstrate trapped electrons at defect sites, which is of help for a better understanding of the bound magnetic polaron mechanism. These observations and the corresponding mechanisms responsible for the ferromagnetism enhancement would advance the insight into the controversial magnetic behaviors in Co:ZnO system.

DOI: 10.1103/PhysRevB.76.045215 PACS number(s): 75.70.Ak, 78.70.Dm, 75.80.+q

I. INTRODUCTION

Diluted magnetic semiconductors (DMSs) have received much attention within the fast emerging field of spintronics.[1] Following the theoretical prediction of room-temperature ferromagnetism ascribed to carrier-mediated mechanism in ZnO-based DMSs,[2] transition-metal (TM)-doped ZnO have been researched intensively to achieve magnetic ordering above room temperature and promising magnetotransport properties.[3–8] However, although Ueda *et al.*[3] reported ferromagnetism at 300 K in some of Co:ZnO films, the reproducibility was less than 10%. Also, both ferromagnetism[3–6] and paramagnetism[6,9] have been observed in doping ZnO for TM^{2+} substitution at Zn^{2+} and magnetic clusters, respectively. In this rather contradictory situation, several recent mechanisms have been reported to reexamine the origin of magnetic ordering in these systems, such as Zn diffusion into the Mn oxide,[10] bound magnetic polaron (BMP) mechanism concerning defects,[11] and the concentrations of oxygen vacancies (or Zn interstitials).[12,13] Yet there is an ongoing debate about these systems. Even more ambiguously, distinct results are frequently obtained in rather similar TM-doped ZnO films.[6,9] To elucidate the confusion, *ab initio* calculations predict that a competition between ferromagnetic and antiferromagnetic coupling exists in DMSs, which is sensitive to magnetic ground states.[14,15]

Previous studies suggest that the magnetic behavior of DMSs appears to be dependent on preparation conditions, such as the doping concentration, substrate temperature, and oxygen partial pressure.[3–6,16–18] However, few or no direct substrate-dependent magnetization has been published on DMSs. The closest work is a review in which the statistic data imply that magnetization in $Co:TiO_2$ films is related to the crystal structures and the substrates.[6] As a matter of fact, some special substrates, such as ferroelectric and piezoelectric crystals and conducting perovskite oxides, are persistent to play an important role in the growth of thin films with considerable magnetotransport and multiferroic properties.[19,20] Moreover, a study of the substrate-dependent magnetization in DMSs films not only provides an insight into the inconsistent magnetic behaviors of DMSs from a theoretical viewpoint, but also serves as a reference for substrate selections in sprintronics for technical purposes.

In this work, we have studied a series of 4 at. % Co-doped ZnO films prepared by direct current (dc) reactive magnetron cosputtering on ferroelectric and piezoelectric crystals, some other single crystals, and amorphous glass substrates to provide an insight into the role of the slight dissimilarity of local Co structure and ground states induced by substrates on magnetic ordering of DMS films.

II. EXPERIMENT AND CALCULATION

4 at. % Co-doped ZnO films were deposited by dc reactive magnetron cosputtering. The substrates are 128° *Y*-*X*$LiNbO_3$ (128LN), 64° *Y*-*X*$LiNbO_3$ (64LN), and 36° *Y*-*X*$LiTaO_3$ (LT) ferroelectric crystals, SiO_2(101) piezoelectric crystal, some other single crystals [e.g., Al_2O_3(001), Si(111), and NaCl(100)], and amorphous glass. The base pressure of the sputter deposition chamber was 4×10^{-6} Torr, and the working pressure was a mixture of argon (2.5×10^{-3} Torr) and oxygen (4.2×10^{-3} Torr). A considerably low substrate temperature of ~200 °C was used in the film deposition process.[18] The film structure and crystalline quality were characterized by x-ray diffraction (XRD) and reflection high-energy electron diffraction (RHEED). High resolution transmission electron microscopy (HRTEM) imaging, selected area electron diffraction (SAED), and energy-dispersive x-ray spectroscopy (EDS) were used to study the interface bonding, structural characteristics, and Co contents in the films. This was complemented by Rutherford backscattering spectroscopy (RBS) for bulk analysis. X-ray photoelectron spectroscopy (XPS) and Co *K*-edge x-ray-absorption near-edge structure (XANES) were used to determine the valence state and local geometry of the Co dopant

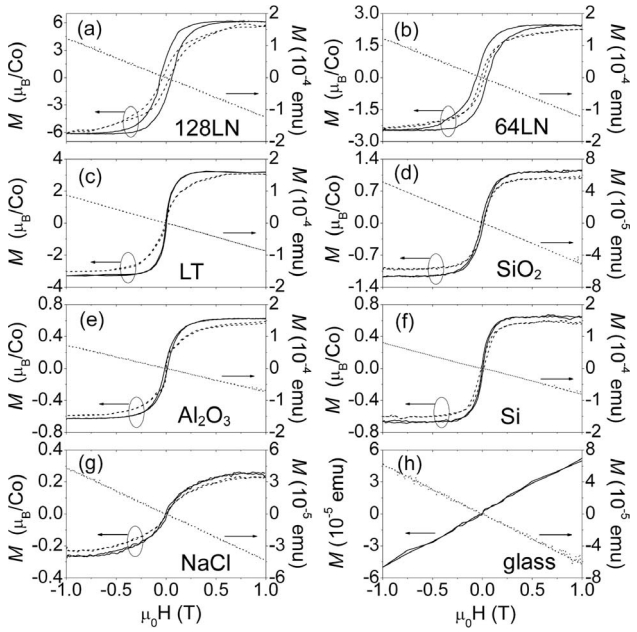

FIG. 1. Magnetization curves measured at room temperature for the Co-doped ZnO films on (a) 128LN, (b) 64LN, (c) LT, (d) SiO_2, (e) Al_2O_3, (f) Si, (g) NaCl, and (h) glass substrates. The magnetization measurements have been performed with magnetic fields applied parallel (solid line) and perpendicular (dashed line) to the plane of the substrate. Magnetization curves (dotted line) of all the blank substrates with a magnetic field parallel to the plane are also shown in the figure.

in the ZnO lattice. Common background subtraction was employed in the data reduction and the data measured in the fluorescence mode were normalized and calibrated to the edge of Co metal foil. The magnetic properties at room temperature were measured using a vibrating sample magnetometer with magnetic fields applied parallel and perpendicular to the plane of the substrates. Inductively coupled plasma (ICP) atomic emission spectra were used to determine the Co contents in the samples after measuring the magnetic properties, and the average magnetic moment per Co atom was then calculated. The total error for the magnetic moment was estimated to be better than 6%.[18]

Co *K*-edge XANES spectra have been calculated via the full multiple-scattering (MS) theory using the *ab initio* self-consistent FEFF 8.2 code[21] with two complementary modes: MS and path analysis by examination of only the most important scattering paths. For the exchange-correlation part of the potential, we have used the energy- and position-dependent optical Hedin-Lundqvist potential with muffin-tin radii overlap of 10% between contiguous spheres to simulate the atomic bond. These conditions have been found to produce good potentials for accurate XANES calculation of complex transition-metal oxides.[21,22]

III. RESULTS AND DISCUSSIONS

Figure 1 shows substrate-dependent magnetization curves of Co:ZnO films, in which the average magnetic moment per Co atom is obtained with respect to ferromagnetism measurement at room temperature and actual Co contents determined by ICP atomic emission spectra. The magnetization measurements have been performed with a magnetic field of 1 T applied parallel and perpendicular to the plane of the substrate, which exhibit that all of our samples show an easy in-plane axis, in agreement with the results of Coey *et al.*[23] in Co:ZnO films grown on *R*-cut sapphire. In the figure, one can see that the substrates have profound influence on the magnetic behaviors of Co:ZnO films. Figure 1(a) is the magnetization versus applied magnetic field (*M-H*) curves for Co:ZnO film on 128LN. Hysteretic behavior is observed, consistent with ferromagnetism, having coercivity and saturation magnetization (M_s) of 61 mT and 6.1 μ_B/Co for the parallel case.[18] A similar giant magnetic moment of 5.9 μ_B/Co was observed by Fitzgerald *et al.*[24] in Co:ZnO system. A pronounced change in the moments is also found in the Co:ZnO films on the same type of substrates, i.e., the Co:ZnO film on 64LN exhibits a comparatively lower moment of 2.5 μ_B/Co, as shown in Fig. 1(b). This phenomenon leads us to consider the origin of magnetization discrepancy on the same type of ferroelectric substrate only with a different cut direction. Interestingly, while room-temperature ferromagnetism with giant magnetic moments per Co atom of 6.1 μ_B, 2.5 μ_B, and 3.2 μ_B is observed in the Co:ZnO films on 128LN, 64LN, and LT ferroelectric crystals, respectively, the film on SiO_2 piezoelectric crystal shows a much lower magnetic moment of 1.1 μ_B/Co [Fig. 1(d)]. Moreover, magnetic moments per Co atom decrease to 0.62 μ_B, 0.66 μ_B, and 0.24 μ_B as the films are deposited on Al_2O_3, Si, and NaCl single crystal, as shown in Figs. 1(e)–1(g), respectively. It is surprisingly noted that the film on glass substrate does not exhibit any signature of ferromagnetism, as indicated by Fig. 1(h). The diamagnetic background of the substrate has been subtracted from all of the magnetization data shown here. Figure 1 also shows the magnetic behaviors of all the corresponding blank substrates, which indicates that the moments in Co:ZnO films do not arise from the substrates.

Although the dependence of the moments of Co:TiO_2 films on substrates is sorted by Janisch *et al.*,[6] such large substrate-dependent magnetization of DMS films for the present data has not been previously reported, which has been highlighted in Fig. 2 with the values of moments per Co atom. It is worth mentioning here that magnetic moments are greatly reduced in $Zn_{0.96}Co_{0.04}O$ films deposited at ~400 °C, thus supporting the previous observation of Sharma *et al.*[4] that high temperature preparation leads to the absence of room-temperature ferromagnetism in Mn:ZnO films. On the other side, the Co:ZnO films deposited on various substrates at ~200 °C have been annealed under the pressure of 5×10^{-6} Torr at 300, 550, and 700 °C for an hour. The room-temperature magnetization measurements show that 300 °C vacuum annealing has a negligible effect on the magnetism of Co:ZnO films, whereas annealing with higher temperature results in a rapid ferromagnetism decrease, accompanied by the enhancement of carrier concentration. For example, it is noted that the giant magnetic moment is vanishing in Co:ZnO/128LN film after annealing at 550 °C, which decreases to ~0.55 μ_B/Co at room temperature.[18] This magnetic transition may be due to an

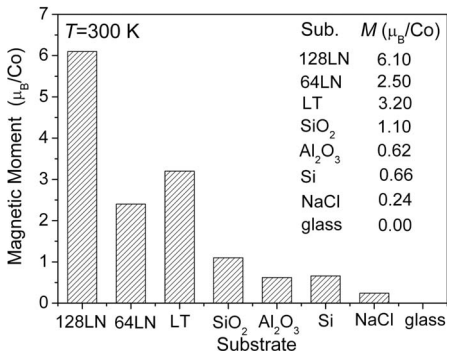

FIG. 2. Plots of room-temperature magnetic moment expressed in Bohr magnetons per Co atom in Co:ZnO films grown on 128LN, 64LN, LT, SiO_2, Al_2O_3, Si, NaCl, and glass substrates. The inset shows the values of moments per Co atom.

evolution of defects which are responsible for mediating room-temperature magnetic ordering and enhanced dopant-dopant associations, leading to progressive orbital moment quenching.[16,18]

To understand the origin of magnetic behavior discrepancy among the Co:ZnO films grown on different substrates, we conducted a systematic study of composition, microstructure, and local chemical information on Co:ZnO films. RBS studies reveal that the film thickness is ~120 nm and the Co contents are ~4 at. %. XRD suggests the formation of a highly aligned phase in all the Co:ZnO films with a *c*-axis preferred orientation, as shown in Fig. 3. Also, very slow scans near the peaks of both hexagonal and cubic cobalt phases reveal no signatures of any kind of additional phases in the films. Concerning the details of Fig. 3, a comparison of (002) diffraction peak of $Zn_{0.96}Co_{0.04}O$ films on different substrates indicates the shift of peak location, which are given in Table I together with the percentage of lattice mismatch between ZnO and various substrates. This shift is most probably due to the matching between the films and substrates. For example, Φ scan of Co:ZnO film on Al_2O_3 obtained from the (101) planes indicates that a 30° rotation between the ZnO and Al_2O_3 *b* axis is presumably due to preferential bonding of Zn atoms with O atoms in Al_2O_3.[25] This lattice matching of ZnO to Al_2O_3 substrate results in epitaxial growth and a (002) diffraction peak located at 34.24°, which is slightly smaller than that of pure ZnO (34.4°) for the doping Co in ZnO lattice, similar to the results reported by Ramachandran *et al.*[5] Moreover, it is found that the (002) peaks located at 33.9° and 33.68° correspond to Co:ZnO films on 128LN and 64LN, respectively. In addition, when the film is deposited on glass, the (002) peak is shifted toward a much smaller angle of 33.52°, leading to a large increase of the out-of-plane lattice parameter. Therefore, from this comparison of Co:ZnO (002) diffraction peak, it can be concluded that the substrate results in lattice parameter changes in Co:ZnO films. Subsequently, these changes would lead to the magnetization variation of Co:ZnO films on various substrates.

HRTEM was performed to investigate the different phases that might have formed in the nanosize range and to determine the state of Co atoms which could not be detected by

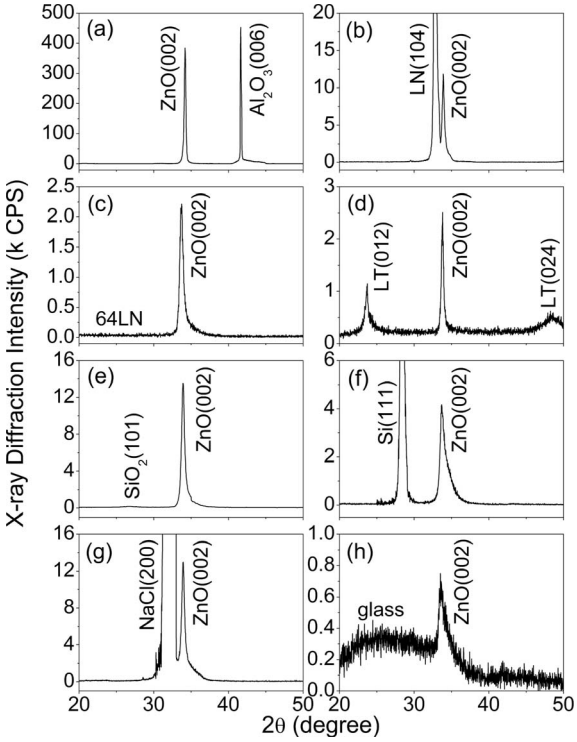

FIG. 3. XRD spectra of the Co-doped ZnO films on (a) Al_2O_3, (b) 128LN, (c) 64LN, (d) LT, (e) SiO_2, (f) Si, (g) NaCl, and (h) glass substrates.

XRD. The typical cross-sectional HRTEM imaging of Co:ZnO film on Al_2O_3 is shown in Fig. 4(a). There is no observation for the presence of Co metal (above 5 at. %) or Co-rich wurtzite clusters in the overall of films. On the contrary, the doping Co are soluble, which are randomly localized over the host lattice. EDS data taken at a number of locations throughout the specimens reveal a solid solution of Co dissolved in ZnO, with Co concentrations ranging from ~3.5 to 4.8 at. % incorporated into the lattice. SAED pattern at the $Zn_{0.96}Co_{0.04}O/Al_2O_3$ interface in the inset of Fig. 4(a) reveals that the orientation relationships between the $Zn_{0.96}Co_{0.04}O$ film and the Al_2O_3 substrate are $(002)_F \| (006)_S$, $(110)_F \| (030)_S$, and $(\bar{1}\,\bar{1}2)_F \| (0\bar{1}2)_S$. Interestingly, epitaxial growth of ZnO-based films on sapphire substrates prepared by a simple and efficient method, i.e., dc reactive magnetron cosputtering, could be an encouraging step for the semiconductor industry concerning ZnO films. Figure 4(b) presents the Co:ZnO film on 128LN substrate. One can see that the (002) planes are not parallel to the surface of the substrates; instead, the pillarlike grains tend to grow in two directions, as marked by the arrows in Fig. 4(b). This growth mode is also supported by our rocking curve recorded around the (002) reflection (not shown). No nanoclusters or precipitates are observed in the film, whereas grain boundaries and some edge dislocations are observed, one of which is highlighted by ⊥ in Fig. 4(b). In addition, the cross-sectional HRTEM imaging from the $[10\bar{1}0]$ zone of Co:ZnO film on SiO_2 substrate exhibits (002) preferred orientation, as shown in Fig. 4(c). Similar to the film on 128LN, one can see numerous grain boundaries and edge disloca-

TABLE I. The percentage of lattice mismatch (δ) between ZnO and Al_2O_3, 128LN, 64LN, LT, SiO_2, Si, and NaCl substrates, the angle 2θ value of the Co:ZnO (002) diffraction peak in Fig. 3, and the distances (Å) of four oxygen atoms (an atom for $d_{Co\text{-}O1}$ and three atoms for $d_{Co\text{-}O2}$) in the first shell from the Co center in Co:ZnO films grown on various substrates for Co *K*-edge XANES calculation.

	Substrate							
	Al_2O_3	128LN	64LN	LT	SiO_2	Si	NaCl	Glass
δ (%)	18.40[a]	36.89	36.89	37.66	33.71	40.10[b]	42.39	
$2\theta_{(002)}$ (deg)	34.24	33.92	33.68	33.82	33.90	33.82	34.04	33.52
$d_{Co\text{-}O1}$ (Å)	1.804	1.823	1.845	1.829	1.825	1.829	1.817	1.859
$d_{Co\text{-}O2}$ (Å)	2.052	2.073	2.097	2.080	2.075	2.080	2.066	2.114

[a]After 30° in-plane rotation.
[b]Reference 25.

tions existing in the film on SiO_2 substrate, and $\perp$ is employed to mark two representative edge dislocations in the figure.

The SAED of Co:ZnO film deposited on NaCl in Fig. 4(d) reveals that the film behave with a hexagonal structure and a perfect texture. The strong arc spots with 12-fold rotational symmetry in the pattern arising from twin crystals can be clearly seen. Pure ZnO twin crystal RHEED patterns were previously obtained by molecular beam epitaxy.[26] On the other side, it is noted that two other panels of identified 12-fold rotational symmetry circle spots are superimposed in Fig. 4(d), one of which is marked by an arrowhead in each panel, as highlighted in the figure. These spots cannot be ascribed to the diffraction of ZnO, Co metal, Zn-Co-O alloys, and Co-based oxides. The Co dopant orderly localizing over the wurtzite lattice and aligning in a regular superstructure from the lattice point of view may be the reason for the appearance of extra 12-fold rotational symmetry circle spots. Further identification of the nature of this structure could be

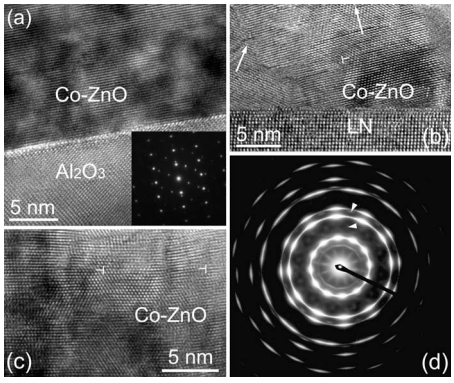

FIG. 4. (a) The HRTEM imaging of $Zn_{0.96}Co_{0.04}O/Al_2O_3$ cross section. The inset is SAED corresponding to the area in (a). (b) Cross-sectional HRTEM imaging of Co:ZnO/128LN. The arrows show two growth directions of (002) planes and one of edge dislocations is marked by white $\perp$. (c) HRTEM imaging from the $[10\bar{1}0]$ zone of $Zn_{0.96}Co_{0.04}O$ grown on SiO_2. Two representative edge dislocations are highlighted by white $\perp$. (d) SAED pattern of Co:ZnO films on NaCl. The arrowheads indicate two representative diffraction spots superimposed on the matrix, which may be introduced by the orderly substituted Co in Co:ZnO films.

available for the understanding of magnetic ordering with orderly substitution, though it is seen to play a negligible role in enhancing the ferromagnetism, that is, the moment is only 0.24 μ_B/Co in Co:ZnO film on NaCl substrate.

XPS was used to characterize the charge state of Co ions in the films, which reveals that Co is in 2+ valence state in Co:ZnO films. However, it is not easy to clarify the Co^{2+} ions (Co^{2+} in wurtzite lattice or CoO) and local Co structure from XPS results. We then have employed Co *K*-edge XANES to obtain local geometry of Co dopant in the lattice and to distinguish local chemical information in Co:ZnO. Co *K*-edge XANES spectra for Co-doped ZnO films on different substrates and various Co-containing materials (Co metal, CoO, and Co_2O_3) are representatively shown in Fig. 5. Following the previous concept that Co^{2+} replace Zn^{2+} in all the Co:ZnO films on different substrates, one can see all the Co *K*-edge XANES spectra from these films have some common features: the small plateau is observed at $E-E_0=0$ eV (E_0

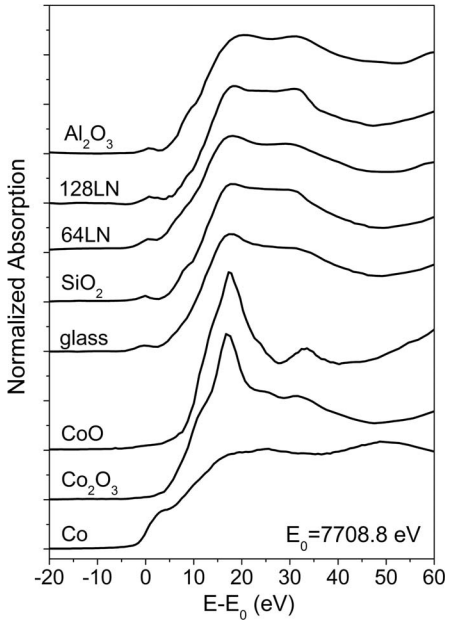

FIG. 5. Representative Co *K*-edge XANES spectra for 4 at. % Co:ZnO films grown on Al_2O_3, 128LN, 64LN, SiO_2, and glass, with reference Co-containing materials: Co metal, CoO, and Co_2O_3.

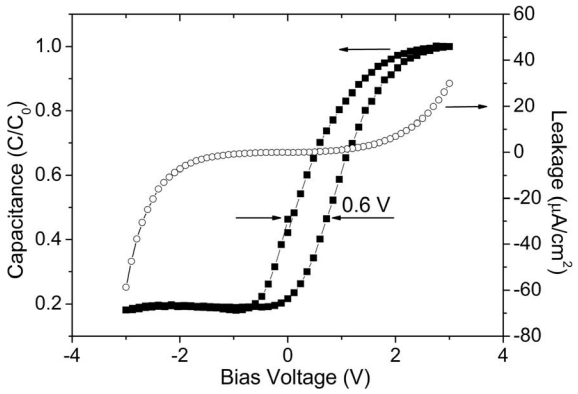

FIG. 6. The typical normalized capacitance (solid squares) and leakage current (open circles) as a function of voltage measured for ~120 nm thick $Zn_{0.96}Co_{0.04}O$ films.

=7708.8 eV) due to the hybridization of Co $3d$/O $2p$ and the core peak is significantly wider than those of Co metal, CoO, and Co_2O_3. On the basis of the previous analysis by our group,[18] there is no evidence of Co metal, CoO, and Co_2O_3 throughout the films, and Co^{2+} is likely to substitute for Zn^{2+}. However, a careful examination of the Co K-edge XANES of Co:ZnO films on different substrates indicates that there are slight differences among the spectra, which will be discussed below.

From the qualitative analysis of XANES spectra, it can be known that the discrepancy of moments cannot be ascribed to the different Co forms in Co:ZnO films grown on different substrates. According to the magnetic measurements discussed above, the moments on ferroelectric crystals are rather robust than those on the other substrates, indicating that ferroelectric substrates play a main role on the ferromagnetism enhancement. It is well known that there is a strong coupling interaction in multiferroic composites fabricated by a combination of ferromagnetic and ferroelectric substances,[27–29] such as the coupling in a $CoFe_2O_4$-$BaTiO_3$ magnetoelectric double layer[28] and an enhanced magnetic moment in multiferroic system.[29] Here, LN and LT substrates show strong room-temperature spontaneous polarization of 70 and 55 $\mu C/cm^2$ and very high ferroelectric transition temperatures T_E of 1483 and 938 K, respectively.[22,30] Therefore, the phenomenon mentioned above is fulfilled, and it is quite natural to suppose that the magnetoelectric coupling mechanism also works in the present case. That is, the magnetic ordering enhancement can, most probably, be attributed to the modulation of the magnetic moment of Co dopant in a structure composed of ferromagnetic films/ferroelectric substrates.

The magnetoelectric coupling between Co:ZnO films/ferroelectric crystals supposed above can also be supported by our electric property measurements of Co:ZnO films, which were performed on a TF Analyser 2000 ferroelectric testing unit. Figure 6 shows a very low leakage current of our patterned $Zn_{0.96}Co_{0.04}O$ films, indicating the highly insulating nature of the films with the resistivity of $\sim 10^8\ \Omega$ cm. The BMP mechanism for highly resistive systems has been reported to understand the magnetic ordering for the absence of carrier-mediated exchange.[11,18] The local ferromagnetism (i.e., BMP) in the present case is then highlighted due to the electron trapped in a defect.[31,32] Fortunately, this is demonstrated by our capacitance-voltage (C-V) measurement, as presented in Fig. 6. One can see that the typical C-V curve of Co:ZnO sample exhibits a hysteresis with a large memory window of 0.6 V, which can be caused by trapped charges at defect sites. Similar phenomena have been recently observed in high-k $HfSiO_4$ and $La_{0.7}Ca_{0.3}MnO_3$ films.[33,34]

On the basis of Ref. 31, the defects may themselves be susceptible to polarization of $PbZr_{0.2}Ti_{0.8}O_3$ layer induced reorganization in a $PbZr_{0.2}Ti_{0.8}O_3/Co:TiO_2/SrRuO_3$ heterostructure, leading to the modification of the room-temperature magnetic moment and coercive field of insulating $Co:TiO_2$ films. Also, the magnetoelectric coupling mainly results from the magnetic-mechanical-electric interaction through the stress and/or strain transforming from one subsystem to another.[35] The diffusion or motion of defects, such as oxygen vacancies, is then driven by the presence of stress and/or strain and by electric field effect[36] arising from spontaneous polarization, to realize an appropriate distance between defects and Co^{2+} and to achieve effective interactions between them. We refer to this process of defect diffusion or motion as the reorganization of defects according to the description by Zhao *et al.*[31] In our case, the defects and the corresponding trapped charges could be significantly modified and reorganized for the sake of strong room-temperature spontaneous polarization of ferroelectric substrates. Subsequently, a donor spin of the well organized defect strongly correlating with Co^{2+} within its orbit can mediate effective interactions between them based on a Heisenberg exchange Hamiltonian. The donors then tend to shape the BMP, coupling Co^{2+} within their orbits, which try to sufficiently spread out to overlap and interact with adjacent BMP to realize magnetic ordering, resulting in rather robust moments, which can be understood with the supercoupling mechanism.[18] This discussion is also supported by the recent observation that the optimized voltage of the piezoelectric substrate can greatly affect the magnetic response of ferromagnetic films.[20] Moreover, our observation is consistent with the theoretical prediction that the modulation of magnetic properties can be realized in DMS/ferroelectric hybrid double quantum wells.[37]

On the other hand, the reorganization of the defects could be partially performed due to the comparatively weak polarization of SiO_2 piezoelectric substrate. Accordingly, the supercoupling mechanism is discounted at this time for there are no appropriate defects to achieve the exchange interaction between the trapped electron and Co^{2+}, offering a lower moment per Co atom in Co:ZnO film, e.g., 1.1 μ_B/Co. Moreover, although the Co dopant also exhibits 2+ state substituting at Zn^{2+}, the defects randomly distributed would lead to very weak moments or no room-temperature ferromagnetism in Co:ZnO films on other single-crystal substrates (e.g., Al_2O_3, Si, and NaCl) and glass substrate, respectively.

The presence of the reorganization of defects due to magnetoelectric coupling can explain the strong magnetic ordering on ferroelectric substrates; it is, however, not sufficient to elucidate the distinguishable moments of Co:ZnO films on 128LN and 64LN. From the XRD spectra, it is noted that Co:ZnO (002) diffraction peaks on 128LN and 64LN are

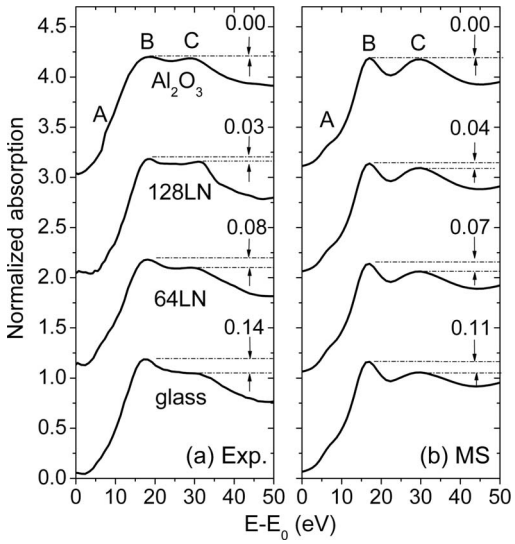

FIG. 7. The experimental and MS calculated XANES spectra of Co:ZnO films grown on Al_2O_3, 128LN, 64LN, and glass, presented from the upper panel to the lower panel.

located at 33.92° and 33.68° (Table I), respectively, indicating an increase of lattice parameter up to 1.2% and a slight dissimilarity of local Co geometry in Co:ZnO. Fortunately, XANES, and its interpretation, is currently of great interest due to its promise of providing local chemical information in complex materials, and it is sensitive to ground-state electronic structure.[21,22] The experimental Co *K*-edge XANES spectra of Co:ZnO films are compared in Fig. 7 with the *ab initio* calculated XANES using full MS theory. These calculated spectra are produced by a cluster which contains 77 atoms within a radius of 6 Å sphere from the central Co atom (which replaces central Zn in ZnO atomic arrangement). It is also noted that the increase of more coordination shells does not lead to significant change in the line shape of the calculated spectra. The atomic arrangement discrimination among the Co:ZnO on Al_2O_3, 128LN, 64LN, and glass is the change of Co-O bond length on the basis of the lattice parameters obtained from XRD results. The atoms and Co-O bond length of the first shell around the center Co are also presented in Table I.

In Fig. 7, one can see that the calculated spectra display three main features accurately replicating those of experimental XANES spectra, denoted by A, B, and C in order of increasing photon energy. We then unambiguously confirm the previous concept that Co^{2+} solute into ZnO lattice sites substitutes for Zn^{2+}.[5,18] Concerning the details of the spectra, for Co:ZnO film on 128LN, it is found that tetrahedron coordination Co photoabsorber is surrounded by the first shell composed of an oxygen atom at 1.820 Å and three oxygen atoms at 2.069 Å, which result in differences of 0.03 and 0.04 between features B and C in normalized absorption for experimental and calculated spectrum, as compared in the second panel of Figs. 7(a) and 7(b), respectively. Similar experimental and simulated XANES spectra have been obtained in Co:ZnO films on SiO_2 substrate. However, for Co:ZnO film on 64LN, the center Co is surrounded by the first shell composed of an oxygen atom at 1.845 Å and three oxygen atoms at 2.097 Å, leading to larger differences of 0.08 and 0.07 for experimental and calculated spectrum, as shown in the third panel of Figs. 7(a) and 7(b), respectively. It is thus found that the slight change of Co-O bond length in Co:ZnO films has a profound influence on the electron movement and scattering in the near range of Co atom. Consequently, electron spin and the corresponding moments could be sensitive to the Co-O bond length. It is very likely that a similar situation is predicted by the previous *ab initio* calculation that the ferromagnetic coupling is affected by the Mn-O bond length in $La_{0.67}Ca_{0.33}MnO_{3-\delta}$ films[19] and that the energy differences between ferromagnetic and antiferromagnetic alignment are very small in Co:ZnO system.[14,38]

On the other hand, a much shorter (longer) Co-O bond length in Co:ZnO films on Al_2O_3 (glass) substrate leads to no discrepancy (e.g., 0.00) and a large distinction (e.g., 0.14 and 0.11 for experimental and calculated spectra, respectively) in normalized absorption, respectively, as shown in Fig. 7. These factors may serve as another reason that results in a weak magnetic coupling in Co:ZnO besides randomly distributed defects. It is this sensitivity of magnetic moment to the Co-O atomic distance that makes Co-containing materials exhibit very complicated magnetic properties ranging from ferromagnetic to nonmagnetic on different substrates. Therefore, the comparison of Co-O atomic distance in Co:ZnO films on various substrates reveals that a suitable Co-O bond length of ~2.069 Å helps enhance magnetization of Co:ZnO films. In addition, in spite of the fact that Co-O bond length has an obvious effect on the magnetic behavior of Co:ZnO films, it is useful to point out here that the reorganization of defects ascribed to magnetoelectric coupling is seen to be a dominant factor, while a suitable Co-O bond length serves as a subordinate one corresponding to the appearance of a large magnetic moment, because the present Co:ZnO insulating films on all the ferroelectric substrates exhibit giant magnetic moments greater than that of metal Co (e.g., 1.7 μ_B/Co), and vice versa.

Although displaying two unusual details, the strong dependence of ferromagnetism on substrates analyzed above may remain generally consistent with the BMP description of ferromagnetism based on the presence of defects in Co-doped ZnO.[11] While defects are responsible for the room-temperature magnetic ordering,[11,18,39] we specialize in the reorganization of defects due to magnetoelectric coupling within the BMP model and a suitable Co-O bond length, which are two detailed ingredients for the enhanced ferromagnetism in insulating Co:ZnO films. Considering that the present films are defective and relative concentration of defects may vary with the substrates, the comparison of ferromagnetism would be more convincing with an analysis of different concentrations of defects on various substrates.

Recalling the observations in the HRTEM cross section, although quantitative concentration of defects cannot be easily obtained, both grain boundaries and edge dislocations are clearly detected in the Co:ZnO films on 128LN and SiO_2 substrates, which are also found in cross-sectional HRTEM imaging of Co:ZnO/Si.[40] These defects can, most probably, be observed in the films on 64LN and LT substrates when the analogous intensity of Co:ZnO (002) XRD peak is taken into account. If ferromagnetism of the films strongly depends on

the concentration of defects, these films would not show magnetization discrepancy with 1 order of magnitude (i.e., 6.1 and 0.66 μ_B/Co for the films on 128LN and Si, respectively) for similar defects detected. In contrast, magnetoelectric coupling likely leads to much higher magnetic moments in Co:ZnO films on ferroelectric crystals than that of the films on the other substrates, as discussed above. Also, the SAED from Co:ZnO film on NaCl shows (002) preferred orientation with twin crystals, corresponding to a low magnetic moment of 0.24 μ_B/Co, which suggests that the defects of twin crystals have a negligible influence on the ferromagnetism enhancement. Furthermore, both Co:ZnO single-crystal film on Al_2O_3 with few defects and polycrystalline films on glass with high concentration of defects possess weak ferromagnetism at room temperature. It is then considered that enhanced ferromagnetism may be not intimately related to the defect contents. The precise identities of the defects are not yet clear, but it is reasonable to associate the reorganization of defects ascribed to magnetoelectric coupling and Co-O bond length to the magnetic ordering. More quantitative analysis of the correlation among the defects, Co-O bond length, and magnetic moment per Co atom needs further study.

It is worth mentioning here that this insight referring to local Co structure appears to apply generally to DMS field. That is, these experimental findings are expected to exploit the possibility of explaining the remarkably important and open question that distinct magnetic behaviors are frequently obtained in similar DMS films, as reported in the past several years.[1–9]

IV. CONCLUSION

In summary, employing complementary characterization, we have systematically studied the influence of substrates on the magnetic behaviors of 4 at. % Co-doped ZnO films. The reorganization of defects attributed to magnetoelectric coupling between Co:ZnO films and ferroelectric crystal substrates may greatly enhance the magnetic ordering. Also, the evidence of the defects with the trapped electrons in Co:ZnO would advance the understanding of bound magnetic polaron mechanism. Furthermore, the moments of Co:ZnO films are seen to be affected by the slight change of Co-O bond length, which is also induced by the matching between films and substrates. These results revealing the intrinsic correlation between DMS films and substrates provide an insight into the common controversy of distinct magnetic behaviors observed in similar films and open a window to a class of promising magnetic materials with strong ferromagnetism at the atomic level.

ACKNOWLEDGMENTS

This work is supported in part by the National Natural Science Foundation of China (Grants Nos. 50325105 and 50371040), the Ministry of Science and Technology of China (Grant No. G2000067207-1), and "The Innovation Plan of Education Ministry of China" in the National Synchrotron Radiation Laboratory.

*Author to whom correspondence should be addressed; panf@mail.tsinghua.edu.cn

[1] I. Žutić, J. Fabian, and S. Das Sarma, Rev. Mod. Phys. **76**, 323 (2004).
[2] T. Dietl, H. Ohno, F. Matsukura, J. Cibert, and D. Ferrand, Science **287**, 1019 (2000).
[3] K. Ueda, H. Tabata, and T. Kawai, Appl. Phys. Lett. **79**, 988 (2001).
[4] P. Sharma, A. Gupta, K. V. Rao, Frank J. Owens, R. Sharma, R. Ahuja, J. M. Osorio Guillen, B. Johansson, and G. A. Gehring, Nat. Mater. **2**, 673 (2003).
[5] S. Ramachandran, A. Tiwari, and J. Narayan, Appl. Phys. Lett. **84**, 5255 (2004).
[6] R. Janisch, P. Gopal, and N. A. Spaldin, J. Phys.: Condens. Matter **17**, R657 (2005).
[7] Q. Xu, L. Hartmann, H. Schmidt, H. Hochmuth, M. Lorenz, R. Schmidt-Grund, C. Sturm, D. Spemann, and M. Grundmann, Phys. Rev. B **73**, 205342 (2006).
[8] Q. Xu, L. Hartmann, H. Schmidt, H. Hochmuth, M. Lorenz, R. Schmidt-Grund, C. Sturm, D. Spemann, and M. Grundmann, J. Appl. Phys. **100**, 013904 (2006).
[9] T. Fukumura, H. Toyosaki, and Y. Yamada, Semicond. Sci. Technol. **20**, S103 (2005).
[10] D. C. Kundaliya, S. B. Ogale, S. E. Lofland, S. Dhar, C. J. Metting, S. R. Shinde, Z. Ma, B. Varughese, K. V. Ramanujachary, L. Salamanca-Riba, and T. Venkatesan, Nat. Mater. **3**, 709 (2004).
[11] J. M. D. Coey, M. Venkatesan, and C. B. Fitzgerald, Nat. Mater. **4**, 173 (2005).
[12] S. Ramachandran, J. Narayan, and J. T. Prater, Appl. Phys. Lett. **88**, 242503 (2006).
[13] N. Khare, M. J. Kappers, M. Wei, M. G. Blamire, and J. L. MacManus-Driscoll, Adv. Mater. (Weinheim, Ger.) **18**, 1449 (2006).
[14] E.-C. Lee and K. J. Chang, Phys. Rev. B **69**, 085205 (2004).
[15] M. H. F. Sluiter, Y. Kawazoe, P. Sharma, A. Inoue, A. R. Raju, C. Rout, and U. V. Waghmare, Phys. Rev. Lett. **94**, 187204 (2005).
[16] S. B. Ogale, R. J. Choudhary, J. P. Buban, S. E. Lofland, S. R. Shinde, S. N. Kale, V. N. Kulkarni, J. Higgins, C. Lanci, J. R. Simpson, N. D. Browning, S. Das Sarma, H. D. Drew, R. L. Greene, and T. Venkatesan, Phys. Rev. Lett. **91**, 077205 (2003).
[17] S. Das Sarma, E. H. Hwang, and A. Kaminski, Phys. Rev. B **67**, 155201 (2003).
[18] C. Song, K. W. Geng, F. Zeng, X. B. Wang, Y. X. Shen, F. Pan, Y. N. Xie, T. Liu, H. T. Zhou, and Z. Fan, Phys. Rev. B **73**, 024405 (2006).
[19] W. Zhang, X. Wang, M. Elliott, and I. W. Boyd, Phys. Rev. B **58**, 14143 (1998).
[20] W. Eyckmans, G. Borghs, and J. de Boeck, *Interfacial Engineering for Optimized Properties III*, MRS Symposia Proceedings

No. 819 (Materials Research Society, Pittsburgh, 2004), p. 147.
[21] A. L. Ankudinov, B. Ravel, J. J. Rehr, and S. D. Conradson, Phys. Rev. B **58**, 7565 (1998).
[22] C. Song, F. Zeng, Y. X. Shen, K. W. Geng, Y. N. Xie, Z. Y. Wu, and F. Pan, Phys. Rev. B **73**, 172412 (2006).
[23] J. M. D. Coey, M. Venkatesan, C. B. Fitzgerald, L. S. Dorneles, P. Stamenov, and J. G. Lunney, J. Magn. Magn. Mater. **290-291**, 1405 (2005).
[24] C. B. Fitzgerald, M. Venkatesan, J. G. Lunney, L. S. Dorneles, and J. M. D. Coey, Appl. Surf. Sci. **247**, 493 (2005).
[25] Ü. Özgür, Ya. I. Alivov, C. Liu, A. Teke, M. A. Reshchikov, S. Doğan, V. Avrutin, S.-J. Cho, and H. Morkoç, J. Appl. Phys. **98**, 041301 (2005).
[26] K. Sakurai, M. Kanehiro, K. Nakahara, T. Tanabe, Shizuo Fujita, and Shigeo Fujita, J. Cryst. Growth **214–215**, 92 (2000).
[27] A. M. J. G. van Run, D. R. Terrell, and J. H. Scholing, J. Mater. Sci. **9**, 1710 (1974).
[28] H. Zheng, J. Wang, S. E. Lofland, Z. Ma, L. Mohaddes-Ardabili, T. Zhao, L. Salamanca-Riba, S. R. Shinde, S. B. Ogale, F. Bai, D. Viehland, Y. Jia, D. G. Schlom, M. Wuttig, A. Roytburd, and R. Ramesh, Science **303**, 661 (2004).
[29] Z. Cheng, X. Wang, C. V. Kannan, K. Ozawa, H. Kimura, T. Nishida, S. Zhang, and T. R. Shrout, Appl. Phys. Lett. **88**, 132909 (2006).
[30] A. N. Morozovska and E. A. Eliseev, Phys. Rev. B **73**, 104440 (2006).
[31] T. Zhao, S. R. Shinde, S. B. Ogale, H. Zheng, T. Venkatesan, R. Ramesh, and S. Das Sarma, Phys. Rev. Lett. **94**, 126601 (2005).
[32] M. Venkatesan, C. B. Fitzgerald, J. G. Lunney, and J. M. D. Coey, Phys. Rev. Lett. **93**, 177206 (2004).
[33] J. Zhu, Z. G. Liu, and Y. Feng, J. Phys. D **36**, 3051 (2003).
[34] D. S. Shang, Q. Wang, L. D. Chen, R. Dong, X. M. Li, and W. Q. Zhang, Phys. Rev. B **73**, 245427 (2006).
[35] J. P. Zhou, H. C. He, Z. Shi, and C. W. Nan, Appl. Phys. Lett. **88**, 013111 (2006).
[36] N. Chandrasekhar, Oriol T. Valls, and A. M. Goldman, Phys. Rev. Lett. **71**, 1079 (1993).
[37] N. Kim, H. Kim, J. W. Kim, S. J. Lee, and T. W. Kang, Phys. Rev. B **73**, 033318 (2006).
[38] N. A. Spaldin, Phys. Rev. B **69**, 125201 (2004).
[39] P. V. Radovanovic and D. R. Gamelin, Phys. Rev. Lett. **91**, 157202 (2003).
[40] X. J. Liu, C. Song, F. Zeng, X. B. Wang, and F. Pan, J. Phys. D **40**, 1608 (2007).